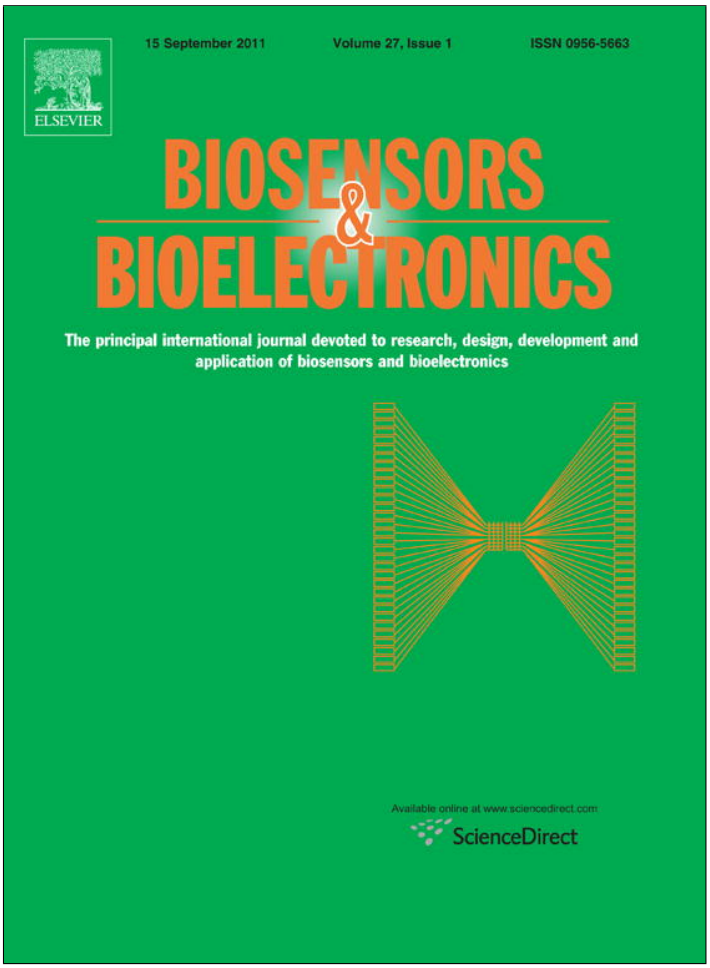

Biosensors and Bioelectronics 27 (2011) 71–76

Contents lists available at ScienceDirect

Biosensors and Bioelectronics

journal homepage: www.elsevier.com/locate/bios

A highly sensitive disposable immunosensor through direct electro-reduction of oxygen catalyzed by palladium nanoparticle decorated carbon nanotube label

Chuan Leng[a], Jie Wu[a], Qiunan Xu[a], Guosong Lai[a], Huangxian Ju[a,*], Feng Yan[b,**]

[a] State Key Laboratory of Analytical Chemistry for Life Science, Department of Chemistry, Nanjing University, Nanjing 210093, PR China
[b] Jiangsu Institute of Cancer Prevention and Cure, Nanjing 210009, PR China

ARTICLE INFO

Article history:
Received 9 May 2011
Accepted 13 June 2011
Available online 21 June 2011

Keywords:
Biosensor
Immunosensor
Immunoassay
Carbon nanotube
Palladium nanoparticles
Screen-printed electrode

ABSTRACT

A palladium nanoparticle decorated carbon nanotube was designed as a label for preparation of a highly sensitive disposable immunosensor. The immunosensor was constructed by assembling the capture antibody on gold nanoparticles decorated graphene nanosheets modified screen printed carbon working electrode. With a sandwich immunoassay mode, the palladium nanoparticle decorated carbon nanotubes were captured to the immunocomplex and showed strong electrocatalytic activity toward oxygen reduction. The use of carbon nanotube carrier offered a high amount of palladium nanoparticles on each immunoconjugate, hence amplified the detectable signal from the electro-reaction of dissolved oxygen. The graphene nanosheets and gold nanoparticles improved the electronic conductivity and the hydrophilicity of electrode surface for immobilization of the capture antibody, respectively. Under optimal conditions, a linear detection range from 50 pg/mL to 10 ng/mL and a limit of detection of 44 pg/mL (0.3 pM) were achieved for human IgG. Using dissolved oxygen as a signal reporter, the detection process avoided deoxygenation. The immunosensor showed acceptable stability, precision and accuracy, indicating potential applications in clinical diagnostics.

1. Introduction

Immunoassay is one of the most important analytical techniques for quantitative detection of proteins due to the highly specific binding of antigens and antibodies. Besides immunoassay methods based on fluorescence, chemiluminescence, surface plasmon resonance and quartz crystal microbalance, electrochemical immunoassay has also attracted considerable attention for its intrinsic advantages such as good portability, low cost and high sensitivity (Li et al., 2008). Therefore, various electrochemical immunosensors, particularly amperometric immunosensors, have been developed for analysis of proteins (Wilson, 2005; Das et al., 2006; Wu et al., 2006; Laboria et al., 2010).

Currently, high sensitivity has become one of the main goals in development of immunoassay methods. A number of recent reports on immunoassay with ultrasensitive detection property focus on nanomaterial-based signal amplification strategies, such as biocatalysis (Das et al., 2006, 2007; Chen et al., 2007; Selvaraju et al., 2008), nano-carrier based signal enhancement (Ambrosi et al., 2007; Cui et al., 2008; Tang and Ren, 2008; Tang et al., 2008) and rolling circle amplification (Ou et al., 2009; Cheng et al., 2010). Among these nanomaterials, functional carbon nanotubes (CNTs) are particularly attractive in signal amplified immunoassays due to their huge surface area-to-weight ratio for loading enzymes including horseradish peroxide (Yu et al., 2006; Bi et al., 2009; Malhotra et al., 2010). However, the horseradish peroxide-based immunoassays need a deoxygenation process and nitrogen atmosphere to exclude the interference of dissolved oxygen in electrochemical detection (Wu et al., 2006; Cui et al., 2008; Tang et al., 2008), which limits the clinical application of these methods, particularly in point-of-care diagnosis.

Substitute methods to avoid the deoxygenation process are to use glucose oxidase (Lai et al., 2009), gold nanoparticles (AuNPs) (Dequaire et al., 2000; Ho et al., 2010; Leng et al., 2010) or silver nanoparticles (Ting et al., 2009) as labels to develop new immunosensing strategies. When AuNPs are used for this purpose, they are firstly chemically oxidized in Br_2 (Dequaire et al., 2000) or electrochemically oxidized in HCl (Ho et al., 2010; Leng et al., 2010), and then reduced to produce the detectable signal. Another strategy is to make use of the catalytic activity of metal nanoparticles such as palladium nanoparticles (PdNPs) (Polsky et al., 2007) toward the reduction of dissolved oxygen. After PdNPs were chemically deposited on gold nanoparticle labeled antibody, the labeled antibody was used for immunoassay by measuring the PdNPs catalyzed oxygen reduction signal. This work used PdNPs to functionalize CNTs and designed a novel electrochemical immunosensing strategy without need of deoxygenation. The high loading ability of

* Corresponding author. Tel.: +86 25 83593593; fax: +86 25 83593593.
** Corresponding author. Tel.: +86 25 83283401; fax: +86 25 83283480.
E-mail addresses: hxju@nju.edu.cn (H. Ju), yanfeng2007@sohu.com (F. Yan).

0956-5663/$ – see front matter © 2011 Elsevier B.V. All rights reserved.
doi:10.1016/j.bios.2011.06.017

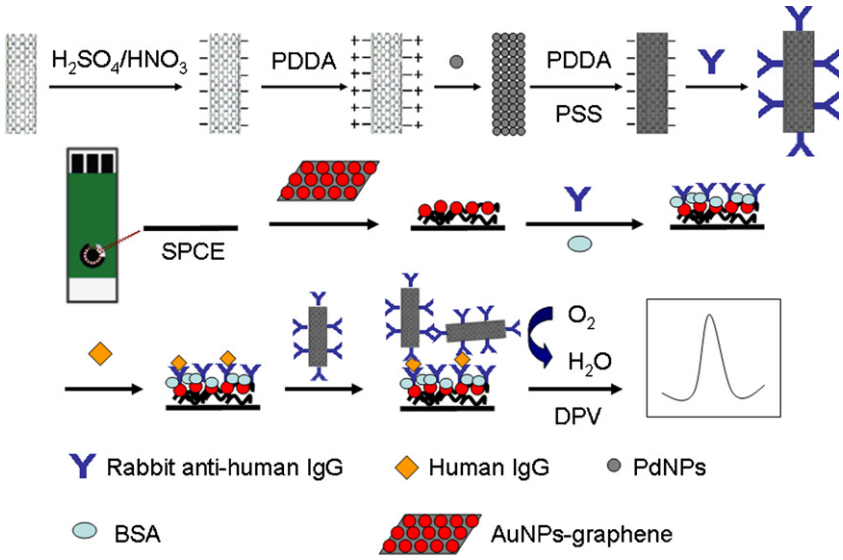

Fig. 1. Schematic representation of the sensitive electrochemical immunoassay using PdNP–CNTs as label.

CNTs introduced numerous nanoparticles with catalytic activity to a recognition event, thus leading to a highly sensitive immunoassay method.

Although the high catalytic ability of PdNPs decorated CNTs has been explored to develop nonenzymatic biosensors for the detection of glucose (Meng et al., 2009; Chen et al., 2010), formic acid (Chakraborty and Raj, 2010) and hydrazine (Haghighi et al., 2010) in recent 2 years, this work used layer-by-layer assembly, different from the previous preparation methods, to prepare the PdNPs decorated CNTs, and further used this nanocomposite to label the secondary antibody for developing a highly sensitive immunoassay method (Fig. 1). With a sandwich format immunoreaction, the labeled secondary antibody was captured on a newly designed immunosensor, prepared by assembling the capture antibody on AuNPs decorated graphene nanosheets modified screen printed carbon working electrode, for highly efficient electrocatalytic reduction of oxygen. The proposed method could detect protein down to 0.3 pM. The immunosensor showed acceptable stability and fabrication reproducibility, and the assay approach had acceptable precision and accuracy, indicating potential applications in clinical diagnostics.

2. Experimental

2.1. Materials and reagents

Human IgG (HIgG) and polyclone rabbit anti-human IgG antibody (RaHIgG) were purchased from Wuhan Boster Biological Technology Ltd. Poly(diallyldimethylammonium chloride) (PDDA, 20%, w/w in water, MW: 200,000–350,000), poly(sodium 4-styrene-sulfonate) (PSS, MW ≈ 70,000), bovine serum albumin (BSA) were obtained from Sigma–Aldrich Chemical Co. (St. Louis, MO). Multiwalled carbon nanotubes (CNTs, CVD method, purity ≥98%, diameter 20–40 nm, and length 1–2 μm) were purchased from Nanoport Co. Ltd. (Shenzhen, China). Graphene oxide was prepared according to a modified Hummer's method (Hummers and Offeman, 1958). Ultrapure water obtained from a Millipore water purification system (≥18 MΩ, Milli-Q, Millipore) was used in all assays. The clinical serum samples were from Jiangsu Institute of Cancer Research. All other reagents were of analytical grade and used as received. 0.1 M phosphate-buffered saline (PBS) solutions with various pHs were prepared by mixing the stock solutions of NaH_2PO_4 and Na_2HPO_4. PBS (pH 7.4) containing 10 mg/mL BSA was used as the blocking buffer.

2.2. Apparatus

The transmission electron micrograph (TEM) was gained on a JEM-2100 TEM (JEOL, Japan). The ζ potential was measured by a Nano-Z Zetasizer nanoparticle analyzer (Malvern Instruments Ltd., USA). X-ray photoelectron spectroscopic (XPS) measurements were performed with an ESCALAB 250 spectrometer (Thermo-VG Scientific, USA) with an ultrahigh vacuum generator. X-ray diffraction (XRD) was performed with an XRD-6000 X-ray diffractometer (Shimadzu, Japan) using Cu Kα radiation. Reflectance absorption infrared (IR) spectra were recorded on a Vector 22 Fourier transform infrared spectrometer (Bruker Optics, Germany). The Raman spectrum was measured with the excitation wavelength of 514 nm on a Renishaw-inVia Raman microscope (Renishaw, United Kingdom). Differential pulse voltammetric (DPV) measurements were preformed using a CHI 660C electrochemical workstation (CH Instruments Inc., USA).

2.3. Preparation of PdNPs–CNTs label

CNTs were firstly treated with 3:1 H_2SO_4/HNO_3 in sonication for 4 h to obtain carboxylic group-functionalized CNTs. The resulting dispersion was filtered and washed repeatedly with water until pH was about 7.0. The oxidized CNTs were further functionalized with PDDA according to the reported method (Lai et al., 2009). The collected PDDA–CNTs were redispersed in water to a concentration of 0.5 mg/mL.

PdNPs was prepared by a $NaBH_4$ reduction method with citrate ion serving as a stabilizer according to a previous report with slight modification (Liu et al., 2010). Briefly, 100 μL of 0.1 M K_2PdCl_4 and 100 μL of 25 mM sodium citrate were added to 10 mL of H_2O under vigorous stirring, respectively. Dropwise addition of 300 μL of 0.1 M freshly prepared $NaBH_4$ to the above solution caused an instant color change. The resulting black mixture was stirred for an additional 30 min at room temperature to obtain PdNPs. 1 mL of the PdNPs solution was mixed with 120 μL of 0.5 mg/mL PDDA–CNTs. The mixture was then allowed to stand overnight and centrifugate. After the obtained PdNPs–CNTs were washed with water twice, they were redispersed in 1 mL of water for characterizations or in

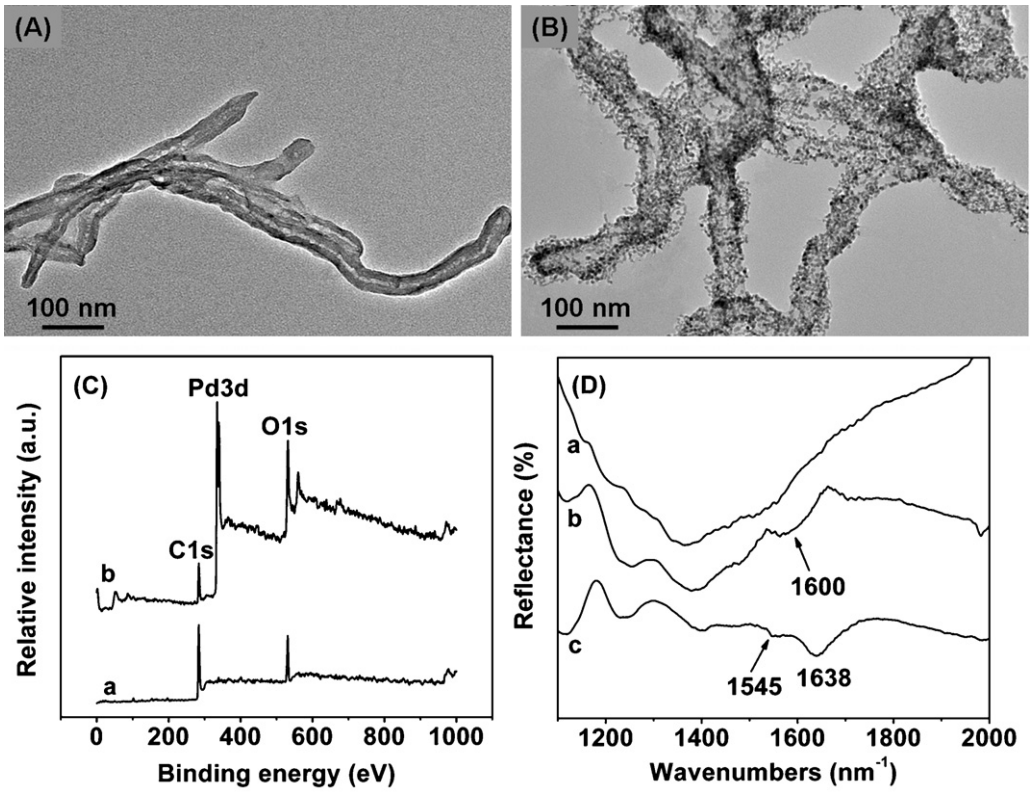

Fig. 2. TEM image of (A) CNTs and (B) PdNPs–CNTs. (C) XPS spectra of (a) PDDA–CNTs and (b) PdNPs–CNTs. (D) Reflectance absorption IR spectra of (a) PdNPs–CNTs, (b) PSS/PDDA–PdNPs–CNTs and (c) PdNPs–CNTs labeled RaHIgG.

0.5 M NaCl solution containing 0.75 mg/mL PDDA for further assembly of PSS and the secondary antibody.

2.4. Preparation of PdNPs–CNTs labeled RaHIgG

Firstly, the mixture solution containing PdNPs–CNTs and PDDA was allowed to shake for 1 h, followed by centrifugation, washing with water thrice and redispersion in 1 mL of 0.5 M NaCl solution containing 0.75 mg/mL PSS. Next, the mixture was allowed to shake for 1 h, and followed by centrifugation, washing with water thrice and redispersion in 1 mL of PBS (pH 6.0) containing 20 μg RaHIgG (Trau et al., 2002; Cai et al., 2008). After shaking for 1 h at room temperature, the mixture was centrifugated and washed with PBS (pH 6.0) to obtain the PdNPs–CNTs labeled RaHIgG, which was redispersed in 200 μL of PBS (pH 6.0) for immunoassay.

2.5. Preparation of the immunosensor

The screen printed carbon electrode (SPCE) system containing carbon working electrode (2 mm in diameter), carbon auxiliary electrode and Ag/AgCl reference electrode was fabricated according to the steps reported previously (Wu et al., 2006). The insulating layer printed around the working area constituted an electrochemical microcell.

Gold nanoparticles decorated graphene nanosheets (AuNPs-graphene) were prepared according to a previous report (Fang et al., 2010). The immunosensor was prepared as follows. First, 1 μL of the prepared AuNPs-graphene was dropped onto the working electrode. After drying, the electrode was washed with water. Then, 1 μL of 0.2 mg/mL RaHIgG in PBS (pH 7.4) was dropped on the AuNPs-graphene modified SPCE and incubated overnight at 4 °C in water vapor saturated environment to allow the assembly of antibody. After washing with water, the electrode surface was incubated with 50 μL of blocking buffer for 30 min at room temperature to suppress the nonspecific adsorption. Finally, the immunosensor was rinsed with water and stored at 4 °C in dry air at dark prior to use.

2.6. Immunoassay procedure

Five microlitres of sample containing HIgG was cast on the immunosensor for 40 min incubation at 25 °C. After a washing step, the immunosensor was incubated with 5 μL of the PdNPs–CNTs labeled RaHIgG for 40 min at 25 °C. After washing with water, 50 μL of PBS (pH 7.4) was dropped on the electrochemical microcell to perform DPV detection from +0.1 V to −0.65 V at 25 °C, with a step potential of 4 mV, a pulse amplitude of 50 mV and a pulse period of 0.2 s.

3. Results and discussion

3.1. Characterization of PdNPs–CNTs labeled RaHIgG

Adsorptive immobilization of antibody molecules onto polyelectrolyte-coated colloidal particles has shown to be a simple and effective means for stably attaching biomolecules and retaining their specific immunorecognition ability (Trau et al., 2002; Cai et al., 2008), thus the PdNPs–CNTs labeled RaHIgG was prepared via layer-by-layer assembly. After positively charged PDDA was adsorbed on negatively charged carboxylated CNTs, the ζ potential changed from −41.6 mV to +45.4 mV. Thus the negatively charged citrate ion protected PdNPs could adsorb on PDDA–CNTs to form PdNPs–CNTs, which led to a change of ζ potential from +45.4 mV to −18.1 mV. For labeling the PdNPs–CNTs to the secondary antibody, positively charged PDDA and negatively charged PSS were assembled onto the nanocomposite successively.

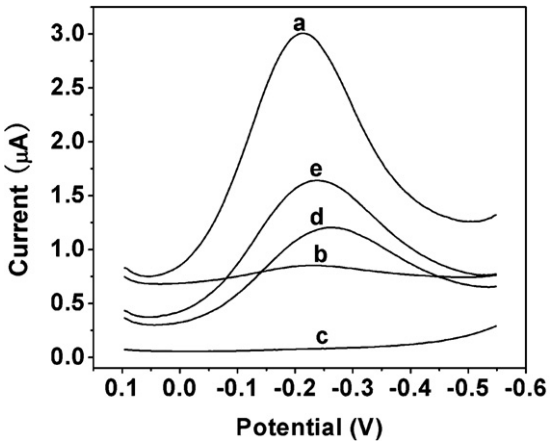

Fig. 3. DPV responses of PdNPs–CNTs labeled RaHIgG modified SPCE in (a) air and (b) N_2 saturated PBS, (c) AuNPs-graphene modified SPCE in air saturated PBS, and SPCEs modified with (d) capture antibody and (e) capture antibody assembled AuNPs-graphene in air saturated PBS after incubation with 1 ng/mL HIgG and PdNPs–CNTs labeled RaHIgG.

During these steps the ζ potential changed to +28.6 and −33.3 mV. As expected, the ζ potential corresponding to each step was in consistence with the charge sign of the substance at the outer layer. According to the previous report (Cai et al., 2008), the best pH for antibody adsorption on PSS was at pH 6.0, the isoelectric point of HIgG molecule, at which HIgG attached to the outmost layer of PSS through mostly hydrophobic interactions (Trau et al., 2002).

Fig. 2A and B displays the TEM images of carboxylated CNTs and PdNPs–CNTs. The carboxylated CNTs obtained by chemical oxidation showed a homogeneous surface and good dispersion (Fig. 2A). Using positively charged PDDA as bridge, negatively charged PdNPs with a 4 nm diameter could electrostatically attach onto the surface of the CNTs and form a compact nanoparticle layer (Fig. 2B).

The successful assembly of the PdNPs on CNTs was also verified by XPS spectra. The spectrum of PDDA–CNTs showed distinct C and O 1s peaks (Fig. 2C, curve a). On the spectrum of PdNPs–CNTs, a new and strong peak at 335.1 eV which represents the Pd3d was observed (Fig. 2C, curve b), indicating the existence of Pd element in the nanocomposite.

Fig. 2D shows the reflectance absorption IR spectra of PdNPs–CNTs, PSS/PDDA–PdNPs–CNTs and PdNPs–CNTs labeled RaHIgG. Compared with the spectrum of PdNPs–CNT (curve a), a new and wide peak around 1600 cm^{-1} was observed for PSS/PDDA–PdNPs–CNTs (curve b), which represents the vibration of C–N bond in PDDA molecules (He et al., 2002). PdNPs–CNTs labeled RaHIgG showed the typical vibration of amide I and amid II of the protein at 1638 and 1545 cm^{-1} (Zhang et al., 2010) (curve c), indicating the successful assembly of RaHIgG on the label.

3.2. Electrocatalytic activity of PdNPs–CNTs labeled RaHIgG

The electrocatalytic activity of PdNPs–CNTs labeled RaHIgG toward oxygen reduction was investigated by DPV measurements. In the studied potential window, the PdNPs–CNTs labeled RaHIgG modified SPCE showed a sensitive DPV peak at −0.22 V after 50 μL of air saturated PBS was cast on the electrode surface (Fig. 3, curve a), while this electrode showed a very weak response in N_2-saturated PBS (Fig. 3, curve b), which was attributed to the reduction of some oxygen-containing groups on CNTs surface, indicating that the strong reduction peak on curve a resulted from the catalytic reduction of dissolved O_2 by PdNPs to H_2O through a four-electron process (Polsky et al., 2007). Contrarily, the AuNPs-graphene modified SPCE did not show any response in both air (Fig. 3, curve c) and N_2 saturated PBS. Thus, the PdNPs–CNTs showed a strong electrocatalytic activity toward the reduction of O_2.

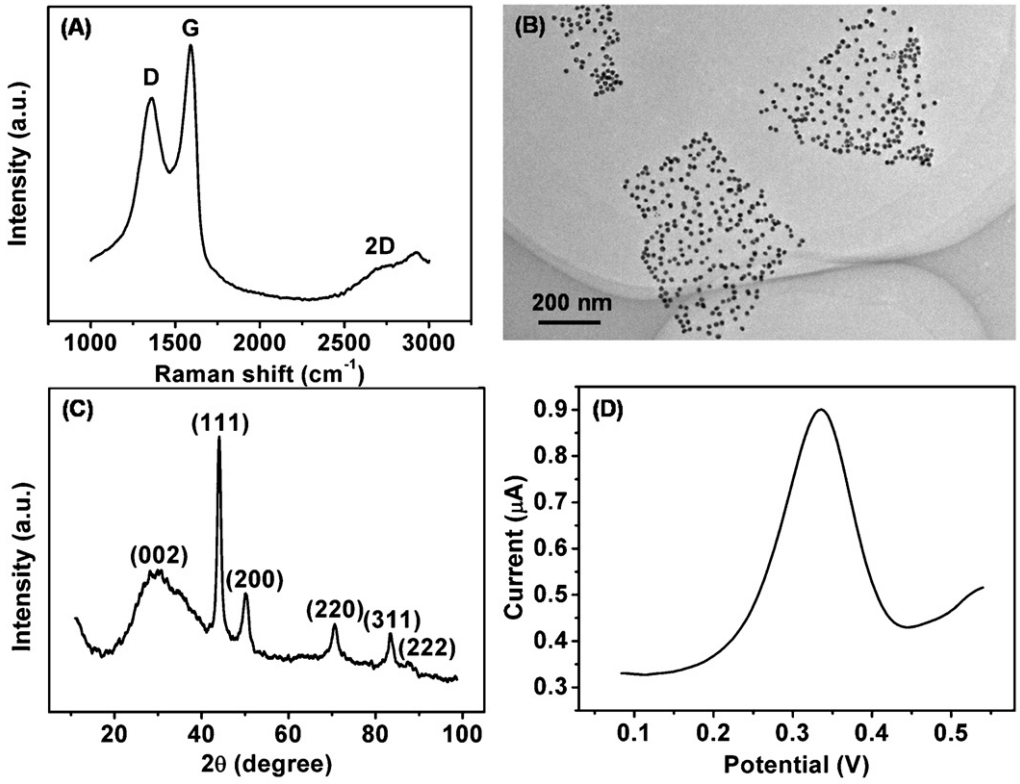

Fig. 4. (A) Raman spectrum of graphene oxide. (B) TEM and (C) XRD images of AuNPs-graphene. (D) DPV response of AuNPs-graphene modified SPCE after electro-oxidation at +1.3 V for 40 s in 0.1 M HCl.

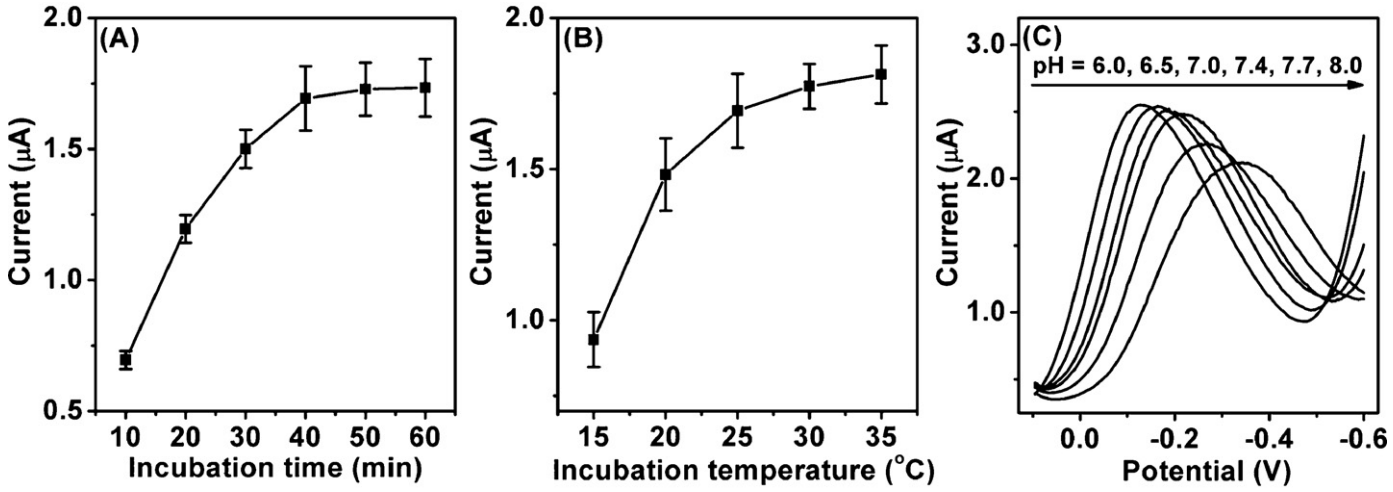

Fig. 5. Effects of (A) incubation time, (B) incubation temperature and (C) pH of the detection solution on DPV response to 5 ng/mL HIgG at the immunosensor.

3.3. Characterization and response of immunosensor to its target

Due to the advantages of graphene nanosheets for capturing more amount of antibody on electrode surface and accelerating the electron transfer (Du et al., 2010; Su et al., 2010) and the good hydrophilicity of AuNPs for immobilization of protein, this work used AuNPs-graphene as immobilization substrate for the assembly of capture antibody. The Raman spectrum of graphene oxide displayed the D band at 1360 cm^{-1}, the G band at 1595 cm^{-1} and a very weak 2D band at 2700 cm^{-1} (Fig. 4A), which were the same as a previous report (Guo et al., 2009), indicating the successful synthesis of the graphene oxide nanosheets. The TEM image of AuNPs-graphene showed that the AuNPs of 15 nm were loaded on the graphene nanosheets (Fig. 4B). The XRD image of AuNPs-graphene showed well-defined crystallinity of AuNPs with five characteristic peaks corresponding to (1 1 1) (2 0 0) (2 2 0) (3 1 1) (2 2 2) crystal faces (Maye et al., 2000) and the characteristic peak of reduced graphene corresponding to (0 0 2) crystal face (Guo et al., 2009) (Fig. 4C). The presence of AuNPs on electrode surface could also be verified by Fig. 4D, which showed a large reduction peak of $AuCl_4^-$ formed during the electro-oxidation of AuNPs at +1.3 V for 40 s in 0.1 M HCl (Leng et al., 2010).

After incubating the RaHIgG assembled SPCE and AuNPs-graphene modified SPCE with 1 ng/mL target HIgG and then PdNPs-CNTs labeled RaHIgG, the PdNPs-CNTs labeled RaHIgG could be attached to electrode surface, thus the resulting electrodes showed the electro-reduction response of dissolved oxygen (Fig. 3, curves d and e). In presence of AuNPs-graphene the DPV response was about one quarter larger than that in absence of AuNPs-graphene, indicating accelerated electron transfer caused by AuNPs-graphene on the SPCE. The catalyzed electro-reduction process and the accelerated electron transfer provided dual signal amplification for highly sensitive immunoassay.

3.4. Optimization of immunoassay conditions

The incubation time is an important parameter affecting analytical performance of immunoassay. At 25 °C, the current response to 5 ng/mL HIgG increased with the increasing incubation time in the sandwich-type immunoassay and reached the maximum value at 40 min (Fig. 5A), indicating saturated binding of the immunoreactions. Therefore, an incubation time of 40 min was selected for the sandwich immunoassay.

The incubation temperature is important during antibody–antigen reaction and also affects analytical performance of immunoassay. With the increasing incubation temperature at an incubation time of 40 min, the current response to 5 ng/mL HIgG increased (Fig. 5B). When the temperature was higher than 25 °C the increase became slow. The signal obtained at 25 °C was over 90% of the maximum signal at 35 °C. Thus, for operational convenience, 25 °C was selected as the incubation temperature.

The effect of pH on DPV curve was shown in Fig. 5C. The peak potential went negatively as the pH increased from 6.0 to 8.0, while the peak current changed insignificantly in the pH range of 6.0–7.4. As electrocatalytic signal was sufficient for detection in PBS of physiological condition (pH 7.4) which is the most commonly used and environment-friendly, pH 7.4 was selected for detection solution.

3.5. Immunoassay performance

As expected from a sandwich mechanism, with the increasing HIgG concentration, the DPV peak current of the immunosensor after incubation with HIgG and PdNPs–CNTs labeled RaHIgG increased due to the increasing amount of PdNPs (Fig. 6). The calibration plot showed a good linear relationship between the peak current and the logarithm value of the HIgG concentration in the range from 50 pg/mL to 10 ng/mL with a correlation coefficient of 0.998. The limit of detection corresponding to the current signal of 3 times standard deviation (SD) above the mean at a zero standard was 44 pg/mL. The SD was obtained from five current measurements at the zero standard.

3.6. Specificity, reproducibility, stability and applications of the immunosensor

The specificity of the immunosensor was examined by testing the amperometric response toward the interfering substances such as BSA, CEA, AFP and glucose prepared in blank PBS. The responses of blank PBS, 10 mg/mL BSA, 100 ng/mL CEA, 100 ng/mL AFP, 1 mM glucose and 1 ng/mL HIgG were recorded. The signals of the interfering substances (0.020–0.045 μA) were near to that of the blank PBS (0.036 ± 0.01 μA) and much smaller than that of 1 ng/mL HIgG (1.19 ± 0.10 μA), indicating good specificity of the proposed immunosensor.

The inter-assay precision of the immunosensor was evaluated using five chips. The coefficients of variation were 8.3% and 2.6% for

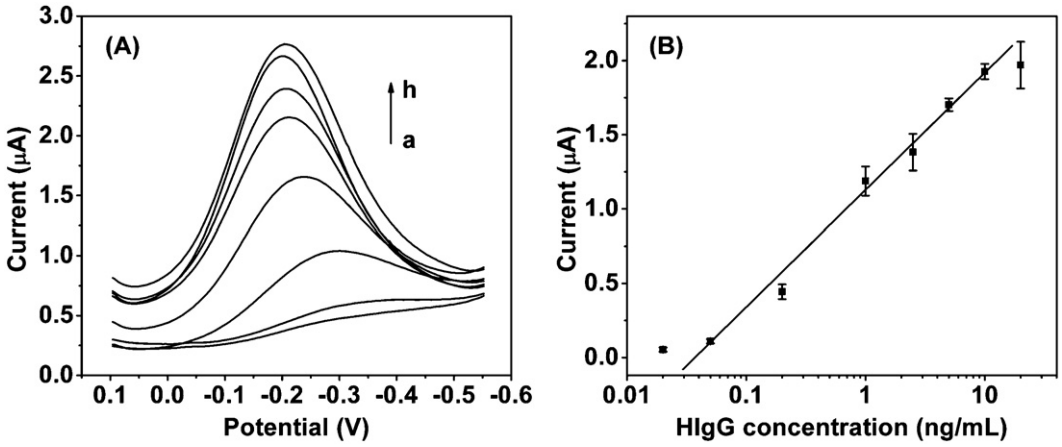

Fig. 6. (A) DPV responses to 0.02, 0.05, 0.2, 1, 2.5, 5, 10, 20 ng/mL HIgG from (a) to (h) using the proposed label and immunosensor. (B) Calibration curve.

1 and 5 ng/mL HIgG, indicating acceptable precision and fabrication reproducibility. After the immunosensors were stored in dry air at dark at 4 °C for a storage period of 2 weeks, the DPV responses were 91.4% of the initial response for HIgG. Thus the storage stability of the immunosensors was acceptable.

After human serum samples were diluted properly with 0.1 M pH 7.4 PBS, different amounts of HIgG were added into the samples for recovery tests. The test results were listed in Table S1. The recoveries were between 90% and 110%, indicating good accuracy of the proposed method for human serum samples.

4. Conclusion

A PdNPs decorated CNTs labeled antibody bioconjugate is prepared via layer-by-layer assembly and used as a trace label for design of an immunoassay method. The immunosensor is fabricated on AuNPs-graphene modified SPCE and the immunoassay is performed in a sandwich format. The PdNPs–CNTs show efficient catalytic activity toward oxygen reduction, resulting in high sensitivity of the immunoassay of HIgG with a relatively wide range. Oxygen as a signal reporter already presents in the detection solution, thus this method does not need a deoxygenation process. The immunosensor has acceptable stability, precision and accuracy, providing a promising potential in simply determination of protein for clinical diagnostics.

Acknowledgements

This work was financially supported by National Basic Research Program of China (2010CB732400), the National Science Fund for Creative Research Groups (20821063) and the projects (20875044, 21075055) from National Natural Science Foundation of China, and Natural Science Foundation of Jiangsu (BK2008014).

Appendix A. Supplementary data

Supplementary data associated with this article can be found, in the online version, at doi:10.1016/j.bios.2011.06.017.

References

Ambrosi, A., Castaneda, M.T., Killard, A.J., Smyth, M.R., Alegret, S., Merkoci, A., 2007. Anal. Chem. 79, 5232–5240.
Bi, S., Zhou, H., Zhang, S.S., 2009. Biosens. Bioelectron. 24, 2961–2966.
Cai, W.Y., Gentle, I.R., Lu, G.Q., Zhu, J.J., Yu, A.M., 2008. Anal. Chem. 80, 5401–5406.
Chakraborty, S., Raj, C.R., 2010. Carbon 48, 3242–3249.
Chen, X.M., Lin, Z.J., Chen, D.J., Jia, T.T., Cai, Z.M., Wang, X.R., Chen, X., Chen, G.N., Oyama, M., 2010. Biosens. Bioelectron. 25, 1803–1808.
Chen, Z.P., Peng, Z.F., Luo, Y., Qu, B., Jiang, J.H., Zhang, X.B., Shen, G.L., Yu, R.Q., 2007. Biosens. Bioelectron. 23, 485–491.
Cheng, W., Yan, F., Ding, L., Ju, H.X., Yin, Y.B., 2010. Anal. Chem. 82, 3337–3342.
Cui, R.J., Huang, H.P., Yin, Z.Z., Gao, D., Zhu, J.J., 2008. Biosens. Bioelectron. 23, 1666–1673.
Das, J., Aziz, M.A., Yang, H., 2006. J. Am. Chem. Soc. 128, 16022–16023.
Das, J., Jo, K., Lee, J.W., Yang, H., 2007. Anal. Chem. 79, 2790–2796.
Dequaire, M., Degrand, C., Limoges, B., 2000. Anal. Chem. 72, 5521–5528.
Du, D., Zou, Z.X., Shin, Y.S., Wang, J., Wu, H., Engelhard, M.H., Liu, J., Aksay, I.A., Lin, Y.H., 2010. Anal. Chem. 82, 2989–2995.
Fang, Y.X., Guo, S.J., Zhu, C.Z., Zhai, Y.M., Wang, E.K., 2010. Langmuir 26, 11277–11282.
Guo, H.L., Wang, X.F., Qian, Q.Y., Wang, F.B., Xia, X.H., 2009. ACS Nano 3, 2653–2659.
Haghighi, B., Hamidi, H., Bozorgzadeh, S., 2010. Anal. Bioanal. Chem. 398, 1411–1416.
He, P.L., Hu, N.F., Zhou, G., 2002. Biomacromolecules 3, 139–146.
Ho, J.A.A., Chang, H.C., Shih, N.Y., Wu, L.C., Chang, Y.F., Chen, C.C., Chou, C., 2010. Anal. Chem. 82, 5944–5950.
Hummers, W.S., Offeman, R.E., 1958. J. Am. Chem. Soc. 80, 1339–11339.
Laboria, N., Fragoso, A., Kemmner, W., Latta, D., Nilsson, O., Botero, M.L., Drese, K., O'Sullivan, C.K., 2010. Anal. Chem. 82, 1712–1719.
Lai, G.S., Yan, F., Ju, H.X., 2009. Anal. Chem. 81, 9730–9736.
Leng, C., Lai, G.S., Yan, F., Ju, H.X., 2010. Anal. Chim. Acta 666, 97–101.
Li, X.M., Yang, X.Y., Zhang, S.S., 2008. TrAC-Trends Anal. Chem. 27, 543–553.
Liu, J.B., Fu, S.H., Yuan, B., Li, Y.L., Deng, Z.X., 2010. J. Am. Chem. Soc. 132, 7279–7281.
Malhotra, R., Patel, V., Vaque, J.P., Gutkind, J.S., Rusling, J.F., 2010. Anal. Chem. 82, 3118–3123.
Maye, M.M., Zheng, W.X., Leibowitz, F.L., Ly, N.K., Zhong, C.J., 2000. Langmuir 16, 490–497.
Meng, L., Jin, J., Yang, G.X., Lu, T.H., Zhang, H., Cai, C.X., 2009. Anal. Chem. 81, 7271–7280.
Ou, L.J., Liu, S.J., Chu, X., Shen, G.L., Yu, R.Q., 2009. Anal. Chem. 81, 9664–9673.
Polsky, R., Harper, J.C., Wheeler, D.R., Dirk, S.M., Rawlings, J.A., Brozik, S.M., 2007. Chem. Commun., 2741–2743.
Selvaraju, T., Das, J., Han, S.W., Yang, H., 2008. Biosens. Bioelectron. 23, 932–938.
Su, B.L., Tang, J.A., Huang, J.X., Yang, H.H., Qiu, B., Chen, G.N., Tang, D.P., 2010. Electroanalysis 22, 2720–2728.
Tang, D.P., Ren, J.J., 2008. Anal. Chem. 80, 8064–8070.
Tang, D.P., Yuan, R., Chal, Y.Q., 2008. Anal. Chem. 80, 1582–1588.
Ting, B.P., Zhang, J., Khan, M., Yang, Y.Y., Ying, J.Y., 2009. Chem. Commun., 6231–6233.
Trau, D., Yang, W.J., Seydack, M., Caruso, F., Yu, N.T., Renneberg, R., 2002. Anal. Chem. 74, 5480–5486.
Wilson, M.S., 2005. Anal. Chem. 77, 1496–1502.
Wu, J., Tang, J.H., Dai, Z., Yan, F., Ju, H.X., El Murr, N., 2006. Biosens. Bioelectron. 22, 102–108.
Yu, X., Munge, B., Patel, V., Jensen, G., Bhirde, A., Gong, J.D., Kim, S.N., Gillespie, J., Gutkind, J.S., Papadimitrakopoulos, F., Rusling, J.F., 2006. J. Am. Chem. Soc. 128, 11199–11205.
Zhang, J., Lei, J.P., Xu, C.L., Ding, L., Ju, H.X., 2010. Anal. Chem. 82, 1117–1122.